Kinetic study of 1,5-cyclooctadiene hydro-isomerization on Pd/pumice catalysts

Dario Duca [a,*], Gianfranco La Manna [b] and Giulio Deganello [a]

[a] *Istituto di Chimica e Tecnologia dei Prodotti Naturali del CNR, Via Ugo La Malfa 153, 90146 Palermo, Italy*
E-mail: dduca@cuc.unipa.it
[b] *Dipartimento di Chimica Fisica, Università di Palermo, Via Archirafi 26, 90123 Palermo, Italy*
E-mail: lamanna@cuc.unipa.it

Received 11 November 1997; accepted 11 March 1998

A new route for obtaining 1,4-cyclooctadiene by catalytic isomerization of 1,5-cyclooctadiene at low temperature in presence of H_2 in a three-phase reactor is presented. Wei, Prater and Silvestri methods are used for the kinetic studies. A comparison of the activity-selectivity patterns of the Pd/pumice catalysts with Pd on silica and Pt and Pd–Pt on pumice catalysts is performed. Although Pt catalysts are not active in the hydro-isomerization of 1,5-cyclooctadiene, the presence of small amount of Pt in Pd/pumice catalysts increases the yield to 1,4-cyclooctadiene. Besides the catalyst characteristics, temperature and H_2 pressure influence the production of 1,4-cyclooctadiene. A mechanism of the process is proposed.

Keywords: 1,4-cyclooctadiene synthesis, hydro-isomerization reactions, kinetics studies, Pd/pumice catalysts

1. Introduction

The detailed knowledge of the catalyzed isomerization of cyclooctadienes has recently become a significant task owing to the industrial interest in *cis-cis*-1,4-cyclooctadiene (1,4-COD) [1]. Only a catalytic route seems to be available for obtaining 1,4-COD in significative yields. Holtrup et al. [1] employed the catalyst system $Ti(OBu)_4/AlEt_3$ directly on 1,5-cyclooctadiene (1,5-COD) reaching up to 30% of 1,4-COD in the isomeric mixture. More recently, Os, Ru, Ir and Rh carbonyls were successfully employed [2]. Higher yields of 1,4-COD were reported with these catalysts in homogeneous as well in heterogeneous processes. All the mentioned approaches, however, needed high reaction temperature (350–520 K).

We have found that 1,4-COD can be obtained in high yield at room temperature by isomerization of 1,5-COD on Pd-based catalysts using a modified three-phase batch reactor [3] at low H_2 pressure. However, the presence of hydrogen (in the reactor) promotes competitive hydrogenation processes affecting the yield of the final products. In order to establish the optimal experimental conditions for the isomerization process, a kinetic study of all the reactions involved is needed.

The overall set of reactions, through the evaluation of the relative kinetic constants, can be studied at different temperatures by Wei, Prater and Silvestri (WPS) [4,5] methods. These, based on simple matrix algebra, require the knowledge of the relative concentrations, at different times, of the substrates involved in the process, irrespective of the actual time values. In some cases, the knowledge of the concentrations of some species at the equilibrium in absence of catalyst is also required.

The equilibrium values of the cyclooctadiene species (CODs) and the thermodynamic properties of the equilibria between 1,5-COD, 1,4-COD and 1,3-cyclooctadiene (1,3-COD) in the gas phase were previously studied by *ab initio* Hartree–Fock calculations [6].

Since the yields of the final products are usually affected by the morphologic characteristics of the catalysts (i.e., particle size and support properties) [7] and the presence of some other metal in the bulk and/or on the surface of the main metal [8], the effects of these factors on the reaction system are also considered in our kinetic study.

2. Experimental

2.1. Catalysts

Table 1 summarizes the catalysts employed and some properties relevant to the work. In the catalyst identification, the first letter indicates the support (P for pumice, S for silica), while the numeric characters are connected with the metal dispersion, equal numbers having comparable metal dispersion. The following letter(s) is(are) referring to the supported metal(s) (D for palladium and T for platinum). The labels $P1_T$ and $P1_{DT}$ correspond to the previously reported [8] Pt_{100} and $Pd/Pt_{95/5}$, whereas $P1_D$, $P2_D$ and $P3_D$ to the W_2, W_6 and W_7 [9,12]. All of them were synthesized by the Yermakov method [13]. The metal dispersion of these catalysts is retained along the time. This property, related to the stability to oxidation (shown under pulse of pure oxygen too [14]), is typical of the metal pumice cat-

* To whom correspondence should be addressed.

Table 1
Main characteristics of the catalysts.

Catalyst	Support	Pd loading (wt%)	Pt loading (wt%)	D_p[a] (Å)	D_x[b]
$P1_D$	pumice[c]	0.108	0.000	29	0.39
$P2_D$	pumice	0.369	0.000	50	0.22
$P3_D$	pumice	1.050	0.000	81	0.14
$S3_D$	silica[d]	1.100	0.000	97	0.11
$P1_{DT}$	pumice	0.518	0.027	32	0.35
$P1_T$	pumice	0.000	0.658	28	0.40

[a] Porod diameter, from SAXS [9].
[b] Normalized dispersion of the metallic phase, from D_p [9].
[c] After standard treatment [9], pumice shows reproducible composition and morphological characteristics [10,11].
[d] Silica gel Davisil (Aldrich), standard grade SS 480 $m^2\,g^{-1}$.

alysts. This unusual characteristic is a consequence of the presence of K^+ and Na^+ ions in the frame of the support which increases the electronic density of the supported metal [8,15]. More details on the synthesis, the structural characteristics and the activity of Yermakov metal pumice catalysts can be found in the quoted [7–12,14–17] papers. $S3_D$, Pd/silica catalyst, was synthesized and characterized according to already reported [9] procedures.

The catalysts of table 1 were selected in order to check the influence on the title reaction of:

- the support;
- the metal loading and dispersion;
- a second metal (Pt) on the Pd catalysts.

2.2. Catalyst activity measurements

All the employed reagents had an analytical grade. Tetrahydrophuran (THF) (Aldrich) was dried and distilled from K under N_2 atmosphere before use. Commercial cyclooctadienes (Aldrich) were purified by fractional distillation from K, passed over activated alumina, and stored at 258 K in Ar. Purity was always checked by GC before use. Hydrogen, GC grade (SOL spa, Palermo), was passed through a BTS catalyst (Fluka) to remove O_2 traces.

The hydro-isomerizations of 1,5-COD were performed employing a new designed three-phase reactor (CFTPR), the schematic drawing of which was previously [3] reported. This, contrary to the usually employed three-phase reactor (TPR) [11,18] which is a closed system, is a continuous-flow reactor and enables to maintain constant the relative gas pressure along all the reaction time also under gas mixture flow. With this apparatus, the 1,5-COD hydro-isomerization was carried out at a total pressure of 1.00 atm varying with He the H_2 pressure from 0.00 to 1.00 atm by two mass-flow controllers (HITECH). At the same experimental conditions (equal temperature, stirring rate, H_2 pressure, amount of catalyst and 1,3-COD concentration in THF), the hydrogenation of 1,3-COD carried out on the above reactors gave activity and selectivity data in the range of the experimental error of the GC analysis (less than 5%). Temperature was controlled ($\pm$0.1 K) by a thermostat. The hydrogen-diffusion effects in the CFTPR were checked on $P3_D$, the most active catalyst, both for 1,3-COD hydrogenation (at 313.15 K) and for 1,5-COD hydro-isomerization (at 308.15 K and hydrogen pressure ranging between 0.25 and 1.00 atm). We observed that the activity values in the conversion of the considered cyclooctadiene, expressed as the number of molecules converted per metallic site per second (TOF), did not change when the stirring rate was higher than 2000 rpm. In our experiments we used 2500 rpm. In this condition, TOF was always found linearly proportional to the catalysts amount. According to Madon et al. [19], we considered our experimental results as being free from any transport influence and, therefore, chemical regime conditions were operating. This guarantees the hydrogen pseudo-steady state on the catalyst surface, necessary [20] for applying the WPS method (see section 3).

The initial reagent concentration in THF was ranging between 1.25×10^{-1} and 5.00×10^{-1} M, and the catalyst amount was arranged in order to have the ratio reagent-moles/metal-atoms between 1000 and 10000. Before the reaction started, the THF-catalyst system was kept under preconditioning [12] for half an hour, being thoroughly stirred with the organic reagents or with H_2. In both cases, when the reaction speed was slow enough (i.e., with the highest reagent-moles/metal-atoms ratios), an induction period was detected.

Kinetic analyses were performed by a DANI 3800 HR-PTV GC equipped with a Supelco capillary column SPB-1701, a DANI 68/10 FID detector and a Shimadzu C-R1B Chromatopac integrator.

After the reactions, as usual when metal/pumice catalysts are employed in three phase hydrogenation in THF [3,8,12], the catalyst retained the same morphological properties and activity.

2.3. Data treatments

The experimental results of the 1,5-COD hydrogenation on $P1_T$ catalyst as well as of the 1,3-COD hydrogenation on all the catalysts were processed employing already reported models [8,12]. The 1,5-COD hydro-isomerization kinetics on Pd and Pd–Pt catalysts were approached by WPS methods (see below). All the codes used in this work (matrix algebra computation and interpolating and fitting programs) are home-made, implemented in FORTRAN and based on *Numerical Recipes* [21].

In the tables, for simplicity, the affix -COD is usually not reported (e.g., 1,5 $\equiv$ 1,5-COD). E represents the cyclooctene (E $\equiv$ COE) and CODs the total amount of the different cyclooctadienes in a reaction mixture.

3. Application of the WPS method

The induction period shown under H_2 and cyclooctadiene preconditioning suggests that the reaction is governed by a surface mechanism [12]. 1,5-COD isomerization does

not occur without H_2 indicating that also the isomerization mechanism must involve hydrogen surface species. Although the formation of β-PdH was claimed [22] in the catalytic processes involving hydrogen species on the Pd surface, it is not important in the present case, since wide-angle X-ray scattering (WAXS) analyses, performed on the $P3_D$ catalyst reused many times under our experimental conditions, did not show any increase in the intensity of the reflection peak (111).

The scheme of the 1,4-COD hydro-isomerization reaction can be represented as follows:

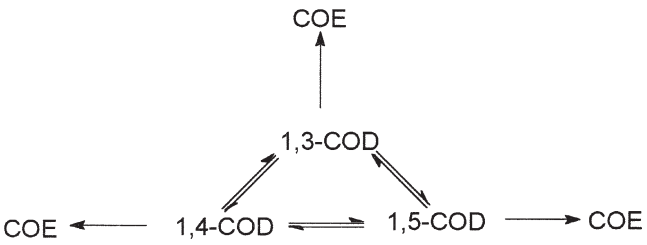

Scheme 1.

Applying Wei, Prater and Silvestri (WPS) methods, the same reaction scheme was successfully employed [20] in the isomerization of n-hexane to 2- and 3-methylpentane on Pt/alumina catalysts in the presence of simultaneous cracking processes. Because of the very low kinetic constant values for the processes 1,3-COD $\rightarrow$ 1, 4-COD and 1,3-COD $\rightarrow$ 1, 5-COD, some difficulties arise from the numerical treatment of the WPS method when applied to the hydro-isomerization depicted in scheme 1. In fact, the kinetic constant values for the processes above are quite lower than those of the other reactions, and the matrix manipulation leads to a divergence of the procedure. This suggests that scheme 1 can be simplified ruling out the isomerization processes involving 1,3-COD. A further simplification can be performed since, as shown in figure 1, starting from 50% of 1,3-COD and 50% of 1,5-COD up to the 40% of the COD mixture conversion, the cyclooctene (COE) formed is essentially obtained from 1,3-COD (line A), irrespective of the conversion of 1,5-COD (line B) and the formation of 1,4-COD (line Γ).

On the basis of these considerations, the following simplified scheme was used in our WPS approach:

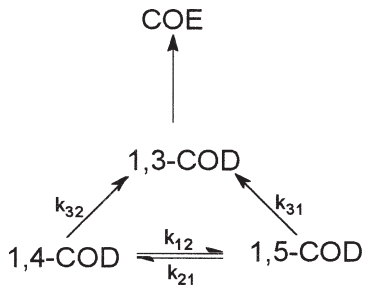

Scheme 2.

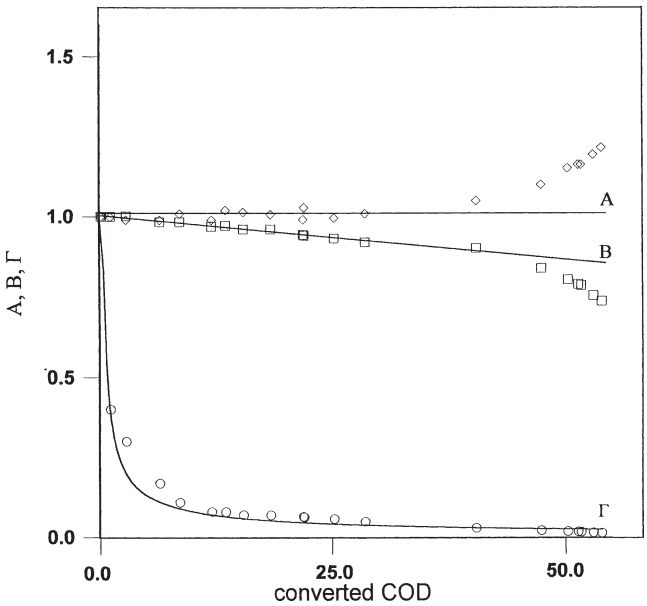

Figure 1. Hydro-isomerization of 1,3-COD and 1,5-COD mixture (50 and 50%) in THF on $P3_D$ catalyst at $T = 298$ K and $p_{H_2} = 1.00$ atm. A = [COE]/[1,3-COD], B = [1,5-COD]/[1,5-COD]° and Γ = [1,4-COD]°/[1,4-COD]. [1,5-COD]° is the 1,5-COD starting concentration and [1,4-COD]° is the 1,4-COD concentration 30 s after the reaction started (this time delay is needed for detecting appreciable amount of the reagent). The curves are joining the experimental points in the range of COD concentrations 0–45%.

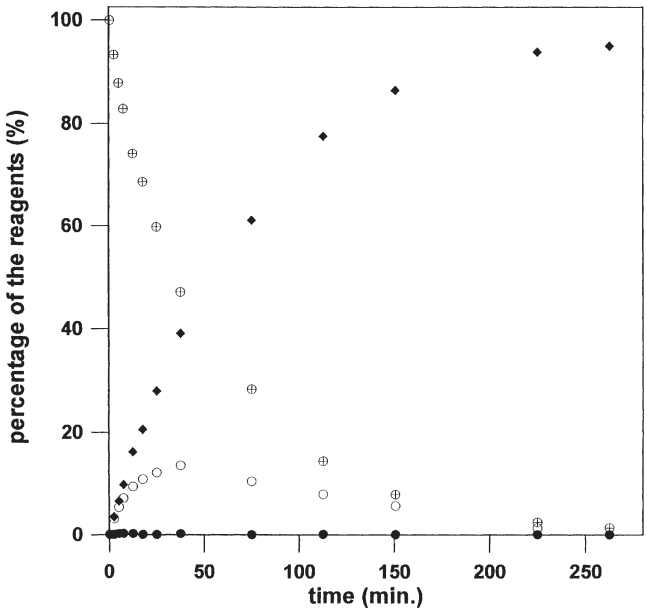

Figure 2. Hydro-isomerization of 1,5-COD in THF on $P3_D$ catalyst at $T = 298$ K and $p_{H_2} = 1.00$ atm. (⊕) Percentage of 1,5-COD, (○) percentage of 1,4-COD, (●) percentage of 1,3-COD and (⧫) percentage of COE.

Let us consider as an example the hydro-isomerization process of 1,5-COD on the $P3_D$ catalyst at 298 K and at a hydrogen pressure of 1.00 atm (figure 2).

The equilibrium composition for the system 1,5-COD $\rightleftharpoons$ 1,4-COD at the conditions above, determined through *ab initio* calculations (0.003/0.997) [6], is requested for deter-

mining the squared matrix **D**:

$$\mathbf{D} = \begin{bmatrix} 0.003 & 0.000 \\ 0.000 & 0.997 \end{bmatrix}.$$

For the system represented by scheme 2, a vector $\mathbf{X}_0$ is defined [4] as

$$\mathbf{X}_0 = \begin{bmatrix} 0.000 \\ 0.000 \\ 1.000 \end{bmatrix},$$

whose components are

$$\begin{bmatrix} \text{1,5-COD} \\ \text{1,4-COD} \\ \text{1,3-COD} + \text{COE} \end{bmatrix}.$$

The dotted line of figure 3, obtained by linear interpolation of the experimental points in the high-conversion region of CODs [4], allows to build the characteristic vector $\alpha_{\mathbf{X}_1}(0)$:

$$\alpha_{\mathbf{X}_1}(0) = \begin{bmatrix} 0.600 \\ 0.400 \\ 0.000 \end{bmatrix},$$

representing the equilibrium composition in the presence of the catalyst. Subtracting the vector $\mathbf{X}_0$ from $\alpha_{\mathbf{X}_1}(0)$ we obtained the characteristic vector $\mathbf{X}_1$:

$$\mathbf{X}_1 = \begin{bmatrix} 0.600 \\ 0.400 \\ -1.000 \end{bmatrix}.$$

The knowledge of the above vectors and the matrix **D** enables to obtain, through simple matrix algebra, the vector $\mathbf{X}_2$ and then the square matrix **X**, whose columns contain the elements of the vectors $\mathbf{X}_0$, $\mathbf{X}_1$ and $\mathbf{X}_2$. In our case,

$$\mathbf{X}_2 = \begin{bmatrix} 1.000 \\ -498.5 \\ 497.5 \end{bmatrix}$$

and

$$\mathbf{X} = \begin{bmatrix} 0.000 & 0.600 & 1.000 \\ 0.000 & 0.400 & -498.5 \\ 1.000 & -1.000 & 497.5 \end{bmatrix}.$$

In the WPS method, the relative rate constant matrix is $\mathbf{K}' = \mathbf{X}\mathbf{\Lambda}\mathbf{X}^{-1}$. $\mathbf{\Lambda}$ is the diagonal square matrix containing the value of the slope referring to a neperian logarithmic plot of known functions of 1,4-COD and 1,5-COD concentrations:

$$\mathbf{\Lambda} = \begin{bmatrix} 0.000 & 0.000 & 0.000 \\ 0.000 & -0.511 & 0.000 \\ 0.000 & 0.000 & -1.000 \end{bmatrix},$$

$$\mathbf{K}' = \begin{bmatrix} -0.511 & 0.001 & 0.000 \\ 0.299 & -0.959 & 0.000 \\ 0.212 & 0.958 & 0.000 \end{bmatrix}.$$

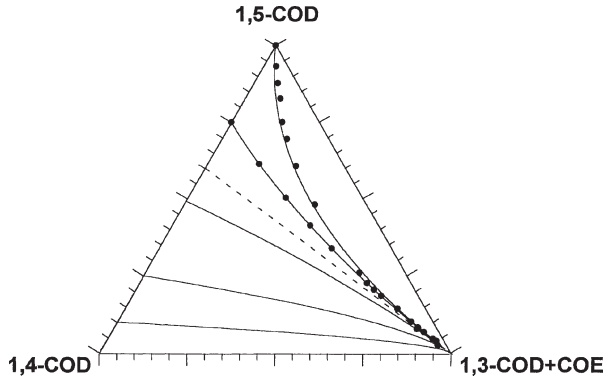

Figure 3. Ternary diagram of the hydro-isomerization of 1,5-COD in THF on $P3_D$ catalyst at $T = 298$ K and $p_{H_2} = 1.00$ atm. (•) Experimental points starting from 100% of 1,5-COD and 75 + 25% of 1,5-COD + 1,4-COD. Dotted line shows the 1,5-COD and 1,4-COD equilibrium values in the considered experimental conditions (see text). Full lines are generated through an interpolation procedure (Runge–Kutta) for different 1,5-COD + 1,4-COD mixtures by using the relative kinetic constants obtained from the WPS method.

$\mathbf{K}'$ matrix contains as (1,2) and (2,1) elements the relative kinetic constants k_{12} and k_{21}, as (3,1) element the relative kinetic constant k_{31} and as (3,2) element the relative constant k_{32} (see scheme 2). The diagonal (1,1) and (2,2) elements represent the overall relative kinetic constants for the disappearance processes of 1,5- and 1,4-COD, respectively. According to the WPS procedure, the signs of the elements on the main diagonal are opposite to those off. Since every multiplication of $\mathbf{K}'$ matrix by an arbitrary number leaves unchanged the relative constant values, we can normalize the $\mathbf{K}'$ matrix to have the first element equal to -1. This allows to obtain directly the TOF values for all the processes involved (see below). The normalized **K** matrix for the considered case is

$$\mathbf{K} = \begin{bmatrix} -1.000 & 0.002 & 0.000 \\ 0.585 & -1.877 & 0.000 \\ 0.415 & 1.875 & 0.000 \end{bmatrix}.$$

4. Results and discussion

Although our experimental conditions (hydrogen pressure, reaction temperature and catalyst used) are very similar to those employed by Carturan et al. [23], in the hydrogenation of 1,3- and 1,5-COD we obtained quite different results. It is likely that the ineffective stirring of the catalytic system [8] is responsible for the lower activity in 1,3-COD hydrogenation as well as for the absence of 1,4-COD along the 1,5-COD hydrogenation reported [23].

Table 2 shows the results of the application of the WPS method for the different experimental conditions here considered. The equilibrium constant for the isomerization 1,4-COD $\rightleftharpoons$ 1,5-COD in different experimental conditions, calculated as k_{21}/k_{12} ratio, are in the range 2×10^{-3}–3×10^{-3}, in good agreement with the *ab initio* results [6]. This shows the self-consistency of the WPS procedure in this case.

Table 2
Relative kinetic constants[a] for the processes involved[b] in the hydro-isomerization of 1,5-COD by WPS method obtained at different experimental conditions.

Catalyst	Temperature (K)	H_2 pressure (atm)	1,5 → 1,3 + 1,4 + E	1,5 → 1,3	1,5 → 1,4	1,4 → 1,3	1,4 → 1,5
$P1_D$	298.15	1.00	1.000	0.397	0.603	1.902	0.002
$P2_D$	298.15	1.00	1.000	0.370	0.630	1.982	0.002
$P3_D$	298.15	1.00	1.000	0.415	0.585	1.875	0.002
$P3_D$	298.15	0.50	1.000	0.323	0.677	2.194	0.002
$P3_D$	298.15	0.25	1.000	0.200	0.800	2.533	0.002
$P3_D$	288.15	1.00	1.000	0.417	0.583	1.729	0.001
$P3_D$	308.15	1.00	1.000	0.466	0.534	1.183	0.002
$S3_D$	298.15	1.00	1.000	0.487	0.513	1.871	0.001
$P1_{DT}$	298.15	1.00	1.000	0.284	0.716	0.998	0.001

[a] The constants are normalized to the overall disappearance process of 1,5-COD.
[b] The hydrogenation of 1,3-COD to COE on Pd and on Pd–Pt catalysts and the hydrogenation of 1,5-COD to COE on Pt catalyst are not considered here since not directly determined by the WPS approach (see text).

Table 3
Processes involved in the 1,5-COD hydro-isomerization: TOF values at different hydrogen pressures and reaction order (α) on $P3_D$ catalyst at 298 K.

H_2 pressure	TOF (s^{-1})					
(atm)	1,3 → E	1,5 → [a]	1,5 → 1,3	1,5 → 1,4	1,4 → 1,3	1,4 → 1,5
1.00	89.4	6.4	2.7	3.7	12.0	0.01
0.50	42.0	3.1	1.0	2.1	6.8	0.006
0.25	19.7	1.5	0.3	1.2	3.8	0.003
α	1.1	1.1	1.5	0.8	0.8	0.9

[a] Overall 1,5-COD conversion.

Table 4
Processes involved in the 1,5-COD hydro-isomerization: TOF values at different temperatures and $p_{H_2} = 1.00$ atm on $P3_D$ catalyst and corresponding activation energy (E_a).

Temperature	TOF (s^{-1})					
(K)	1,3 → E	1,5 → [a]	1,5 → 1,3	1,5 → 1,4	1,4 → 1,3	1,4 → 1,5
288.15	49.9	2.4	1.0	1.4	4.2	0.003
293.15	61.6	–	–	–	–	–
298.15	89.4	6.4	2.7	3.7	12.0	0.01
303.15	121.5	–	–	–	–	–
308.15	162.4	27.9	13.0	14.9	33.0	0.06
313.15	221.4	–	–	–	–	–
E_a ($kJ\,mol^{-1}$)	45.9	90.4	96.1	88.7	78.2	110.2

[a] Overall 1,5-COD conversion.

In order to obtain the TOF values for the different processes involved in the hydro-isomerization reactions, one TOF value for the overall 1,5-COD disappearance processes is needed. This is obtained from the slope of the line representing the conversion of 1,5-COD at initial times (see figure 2, where one of the experimental conditions is considered).

The influence of the hydrogen pressure on the 1,3-COD and 1,5-COD conversion processes, which is summarized by the hydrogen reaction order, is reported in table 3. Only one catalyst at the same temperature is considered. The hydrogen reaction order is obtained by a logarithmic plot of TOF versus hydrogen pressure, assuming a pseudo-zero reaction order for the hydrocarbon [12]. The equal values obtained for the two different overall processes (1.1) suggest that the relative rates are not affected by the hydrogen pressure. Moreover, table 3 shows that, in order to avoid the influence of the related process (1,5-COD → 1,3-COD) on the synthesis of 1,4-COD, it is advisable to work at low hydrogen pressure (below 1.00 atm). This is because the isomerization 1,5-COD → 1,4-COD is characterized by a hydrogen reaction order (0.8) lower than those found for the competitive processes 1,3-COD → COE (1.1) and 1,5-COD → 1,3-COD (1.5).

The analysis of TOF values of both the overall reaction and the elementary steps at different temperatures on the same catalyst and at the same hydrogen pressure gives the apparent activation energy of the involved reaction steps (table 4). The activation energy values show that the disappearance of the CODs in the reaction mixture, occurring

Table 5
TOF values for the processes involved in the 1,5-COD hydro-isomerization on different catalysts at 298 K and $p_{H_2} = 1.00$ atm.

Catalysts	TOF (s^{-1})					
	1,3 → E	1,5 → [a]	1,5 → 1,3	1,5 → 1,4	1,4 → 1,3	1,4 → 1,5
$P1_D$	85.4[b]	1.3	0.5	0.8	2.5	0.003
$P2_D$	90.9[b]	3.1	1.1	1.9	6.1	0.006
$P3_D$	89.4[b]	6.4	2.7	3.7	12.0	0.01
$S3_D$	87.0	12.1	5.9	6.2	22.6	0.02
$P1_{DT}$	3.0[c]	1.7	0.4	1.2	1.7	0.002
$P1_T$	1.0[c]	0.3	–	–	–	–

[a] Overall 1,5-COD conversion.
[b] Data already published [10].
[c] Data already published [8].

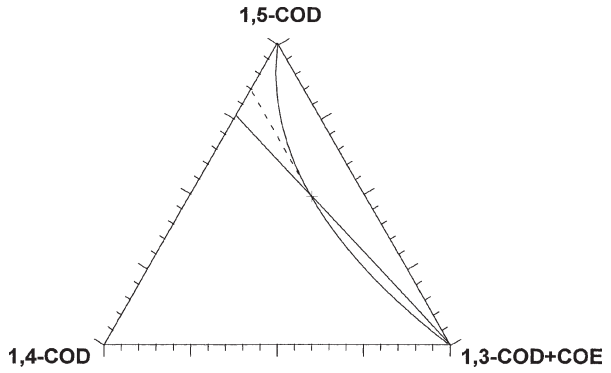

Figure 4. Ternary diagram of the hydro-isomerization of 1,5-COD in THF on $P3_D$ catalyst at $T = 298$ K and $p_{H_2} = 1.00$ atm. Curved and straight line are the reaction and isocline space, respectively (see text), dotted line gives the maximum obtainable 1,4-COD yields for the considered catalytic system.

via the step 1,3-COD → COE, is better prevented at higher temperature.

Table 5 shows TOF values for the 1,3-COD hydrogenation and for the processes involved in the 1,5-COD hydro-isomerization on different catalysts (at same pressure and temperature). Table 5 highlights the difference between Pd- and Pt-based catalysts, the latter not showing any activity in the isomerization processes.

A deeper analysis of the data in the tables 2–5 could certainly suggest a route for reaching the highest 1,4-COD yields in the considered experimental conditions. However, starting from kinetic constant values, the WPS method gives directly the maximum and/or minimum achievable yields of species involved in generic reactions, by the intersection points of the isocline space [4] of the given species with the considered reaction space. In our case, the reaction space is represented by one of the time-independent curves showing the changes of the species concentration in the ternary diagrams (figure 3). The isocline space for a given species σ is determined by $\dot{c}_\sigma = 0$, where $\dot{c}_\sigma$ is the time first derivative of the σ concentration. In our case, the isocline spaces for the different cyclooctadienes are straight lines. The isocline space of 1,4-COD is

$$C_{1,4} = \frac{k_{21}}{k_{12} + k_{32}} C_{1,5},$$

Table 6
Maximum obtainable 1,4-COD yield and corresponding 1,4-COD/CODs ratio in different experimental conditions.

Catalyst	Temperature (K)	H_2 pressure (atm)	1,4 yield (%)	1,4/CODs ratio (%)
$P1_D$	298.15	1.00	16	23
$P2_D$	298.15	1.00	17	24
$P3_D$	298.15	1.00	15	23
$P3_D$	298.15	0.50	18	26
$P3_D$	298.15	0.25	21	28
$P3_D$	288.15	1.00	13	22
$P3_D$	308.15	1.00	20	33
$S3_D$	298.15	1.00	15	23
$P1_{DT}$	298.15	1.00	24	40

with C_i, the concentration of the generic species (i), in the ternary diagram representation. Figure 4 shows the 1,4-COD isocline and reaction space intersection point and the relative 0-slope point [4] of 1,4-COD in a particular experimental condition. The intersection point represents certainly a maximum because, as figure 2 shows, 1,4-COD species have just one maximum along the time path. Using diagrams like that of figure 4, maximum 1,4-COD yield values in the considered experimental conditions were obtained. They are summarized in table 6 along with the corresponding 1,4-COD/CODs ratio. This method for obtaining 1,4-COD is certainly promising since also using much "softer" temperature conditions than those usually employed [1,2] the 1,4-COD/CODs ratios are quite high.

Some evidences already outlined are confirmed by table 6:

- Higher H_2 pressure decreases the selectivity to 1,4-COD (rows 3–5).
- Higher reaction temperatures increases the selectivity to 1,4-COD (rows 3, 6, 7).

Moreover, table 6 shows that the metal loading as well as metal dispersion (rows 1–3, 8) and the nature of the support (rows 3, 8) do not influence the selectivity to 1,4-COD. Finally, the observation of the first and the last row of table 6, where Pd and Pd–Pt catalysts having similar dispersion are considered under the same reaction conditions, seems to suggest that a guest metal, even not active

alone in the 1,5-COD → 1,4-COD isomerization, strongly enhances the selectivity of Pd catalysts to 1,4-COD in the title reaction. Since Pt in this bimetallic Pd–Pt catalyst is almost completely localized on the surface of the host metal (Pd) [24], the increased selectivity to 1,4-COD should be attributed to ensemble size rather than to electronic effects.

5. Conclusions

The full application of the WPS methods to study the hydro-isomerization of 1,5-COD enabled to find the reaction mechanism represented by scheme 2 and showed large capability to investigate 1,4-COD optimization processes.

Although further studies are needed, the synthesis of 1,4-COD via hydro-isomerization of 1,5-COD on metal catalysts seems a promising method. In the development of this method, the following points have to be considered:

- In order to obtain higher 1,4-COD yields, it is advisable to work at low H_2 pressure and high reaction temperature.
- Both the lower H_2 pressure and the higher temperature values decrease the hydrogenation of 1,3-COD with respect to the global cyclooctadiene isomerization processes.
- The support as well as the metal dispersion and loading, at least in the range here considered, do not seem to influence the catalytic activity of the Pd catalyst in the 1,4-COD production.
- Although Pt-supported catalysts are not active in the isomerization processes, the presence of Pt as guest metal on the catalyst surface appears to enhance the yield of 1,4-COD.

References

[1] W. Holtrup, R. Streck, W. Zaar and D. Zerpner, J. Mol. Catal. 36 (1986) 127.
[2] J. Kaspar, M. Graziani, G. Dolcetti, A. Trovarelli and R. Ganzerla, J. Mol. Catal. 48 (1988) 29;
J. Kaspar, M. Graziani, A. Trovarelli and G. Dolcetti, J. Mol. Catal. 55 (1989) 229;
C. Ebert, T. Gianferrara, M. Graziani, J. Kaspar, P. Linda and A. Trovarelli, J. Catal. 124 (1990) 443;
A. Trovarelli, G. Dolcetti, J. Kaspar and M. Graziani, J. Catal. 129 (1991) 288.
[3] D. Duca, L.F. Liotta and G. Deganello, Catal. Today 24 (1995) 15.
[4] J. Wei and C.D. Prater, Adv. Catal. 13 (1962) 203.
[5] C.D. Prater, A.J. Silvestri and J. Wei, Chem. Eng. Sci. 22 (1967) 1587;
A.J. Silvestri, C.D. Prater and J. Wei, Chem. Eng. Sci. 23 (1968) 1191;
A.J. Silvestri, C.D. Prater and J. Wei, Chem. Eng. Sci. 25 (1970) 407.
[6] G. La Manna and D. Duca, J. Mol. Catal. A 111 (1996) 109.
[7] A.M. Venezia, A. Rossi, D. Duca, A. Martorana and G. Deganello, Appl. Catal. A 125 (1995) 113.
[8] G. Deganello, D. Duca, L.F. Liotta, A. Martorana, A.M. Venezia, A. Benedetti and G. Fagherazzi, J. Catal. 151 (1995) 125.
[9] G. Fagherazzi, A. Benedetti, G. Deganello, D. Duca, A. Martorana and G. Spoto, J. Catal. 150 (1994) 117.
[10] M.A. Floriano, A.M. Venezia, G. Deganello, E.C. Svensson and J.H. Root, J. Appl. Cryst. 27 (1994) 271;
D. Duca and G. Deganello, J. Mol. Catal. 112 (1996) 413.
[11] G. Deganello, D. Duca, L.F. Liotta, A. Martorana and A.M. Venezia, Gazz. Chim. Ital. 124 (1994) 229.
[12] G. Deganello, D. Duca, A. Martorana, G. Fagherazzi and A. Benedetti, J. Catal. 150 (1994) 127;
D. Duca, L.F. Liotta and G. Deganello, J. Catal. 154 (1995) 69.
[13] Y.I. Yermakov, Catal. Rev. 13 (1976) 77.
[14] D. Duca, F. Arena, A. Parmaliana and G.Deganello, Appl. Catal. A (1998), in press.
[15] A.M. Venezia, D. Duca, M.A. Floriano, G. Deganello and A. Rossi, Surf. Interface Anal. 18 (1992) 619.
[16] D. Duca, F. Frusteri, A. Parmaliana and G. Deganello, Appl. Catal. A 146 (1996) 269.
[17] G. Fagherazzi, A. Benedetti, A. Martorana, S. Giuliano, D. Duca, and G. Deganello, Catal. Lett. 6 (1990) 263;
A. Martorana, G. Deganello, D. Duca, A. Benedetti and G. Fagherazzi, J. Appl. Cryst. 25 (1992) 31.
[18] E. Santacesaria, P. Wilkinson, P. Babini and S. Carrà, Ind. Eng. Chem. Res. 27 (1988) 780.
[19] J.R. Madon and M. Boudart, Ind. Eng. Chem. Fund. 21 (1982) 438.
[20] I. Surjo and E. Christoffel, J. Catal. 60 (1979) 133.
[21] W.H. Press, S.A. Teukolsky, W.T. Vetterling and B.P. Flammery, in: *Numerical Recipes* (Cambridge University Press, Cambridge, 1992).
[22] A. Janko, W. Palczewska and I. Szymerska, J. Catal. 61 (1980) 267; C.M. Pradier, M. Mazina, Y. Berthier and J. Oudar, J. Mol. Catal. 89 (1994) 211.
[23] G. Carturan and G. Strukul, J. Catal. 57 (1979) 516.
[24] A.M. Venezia, D. Duca, M.A. Floriano, G. Deganello and A. Rossi, Surf. Interface Anal. 19 (1992) 543.